

SURFACE AND STRUCTURAL PROPERTIES OF 3, 5 AND 10A SYNTHETIC ZEOLITES

T M EL-AKKAD, A M KHALIL, G ATTIA and SH NASHED

Department of Chemistry, Faculty of Science, Ain Shams University, Abbasia, Cairo (Egypt)

(Received 12 May 1981)

ABSTRACT

The surface and structural properties of synthetic zeolites thermally treated between 100 and 1000°C were investigated by X-ray, DTA, TG and nitrogen adsorption at -195°C. The zeolites under investigation possess a crystalline structure similar to nepheline, their diffraction patterns completely disappeared on thermal treatment at 800°C due to destruction of the zeolitic lattice. Differential thermal analysis exhibited an endothermic effect centered at about 225°C which may be attributed to dehydration of loosely bound zeolitic water, and two successive exothermic effects, the former was small, centered at 855°C, the latter, which was sharper, appeared at about 920°C. These may be due to evolution of structural water followed by destruction of the zeolite lattice, respectively. Thermogravimetric analysis indicated that the water loss in air exceeded that in vacuum, an effect which is indicative of contraction of the zeolite structure by the action of a high vacuum procedure at elevated temperature.

Nitrogen adsorption studies at -195°C were used as a probe to follow the textural and structural changes due to thermal treatment between 100 and 1000°C. Evolution of the monolayer equivalent using the method of Dubinin Radushkevich gave higher estimated values than those calculated by the BET method. These higher values can be attributed to the influence of the micropore filling of nitrogen in the low pressure region which led to distortion in the shape of the isotherms in the initial pressure region, and hence the evaluation of V_m by the BET method may be considered unreliable in this connection. In general, monolayer equivalents increase with increase in the pretreatment temperature up to 400°C followed by a gradual decrease as the pretreatment temperature increases. The increase in monolayer equivalents may be correlated with the removal of loosely bound water in the intracrystalline cavities or pores, an effect which leads to an increase in the accessibility of the nitrogen molecule. The decrease in nitrogen uptake on samples thermally treated at temperatures higher than 400°C can be attributed to contraction of the zeolite pores by heating in vacuum; an effect which precedes partial collapse of the structure. The marked decrease obtained on thermal treatment at 800°C may be correlated with destruction of the zeolite lattice producing a mixture of different sintered oxides.

INTRODUCTION

Natural and synthetic zeolites, as molecular sieves, are classed among the most important catalysts in view of their micropore texture and extensively large surface area. The most interesting applications of zeolites as molecular sieves are probably the removal of water from gas streams [1], the separation of straight chain paraffins from branched chain hydrocarbons, and in catalytic cracking reactions [2,3]. Many

new species of zeolites have been prepared by Milton et al. [4,5]. The present investigation aims at further elucidating the surface and structural properties of three type A zeolites, namely, 3, 5 and 10A zeolites and their thermal products.

EXPERIMENTAL

Materials

Three zeolites, namely 3, 5 and 10A, were supplied from the chemical laboratory of Carl Roth, OHG-75 Karlsruhe, West Germany.

Apparatus

X-ray analysis

The structure of the zeolites under investigation and their thermal products were studied by X-ray analysis using a Philips type PW 1050 X-ray diffractometer. The patterns were run using Ni filtered K_{α} radiation. The distances (d) were calculated and their relative intensities (I) were compared with standard ASTM data cards [6].

Thermogravimetric analysis (TGA)

Thermogravimetric analysis of the zeolite samples was carried out using an automatic thermobalance, provided by Gebrüder Netzsch, West Germany, the thermograms being obtained at a constant heating rate of $5^{\circ}\text{C min}^{-1}$.

Differential thermal analysis (DTA)

Phase changes accompanying the thermal treatment of the zeolites were studied using an accurate apparatus, locally made with d.c. amplifier (Leeds and Northrup) and a two-channel recorder (type H and B Poly Comp.). The technique adopted followed the recommendation of MacKenzie [7] and McAdie [8].

Adsorption measurements

Adsorption of nitrogen at -195°C on the various zeolite samples was carried out using a conventional volumetric apparatus [9]. Thermal treatment of the original zeolites up to 500°C was carried out in vacuo for 4 h using a tubular furnace, and the rate of heating was adjusted between 2.5 and $3^{\circ}\text{C min}^{-1}$. Thermal treatment at 800 and 1000°C was performed in air for 4 h followed by outgassing for 5 h at a pressure lower than 10^{-4} mm Hg before carrying out nitrogen adsorption measurements.

RESULTS AND DISCUSSION

Figures 1–3 indicate that 3, 5 and 10A synthetic zeolites possess diffraction patterns typical of nepheline [sodium aluminium silicate ($\text{Na}_3\text{KAlSi}_4\text{O}_{16}$)] which has

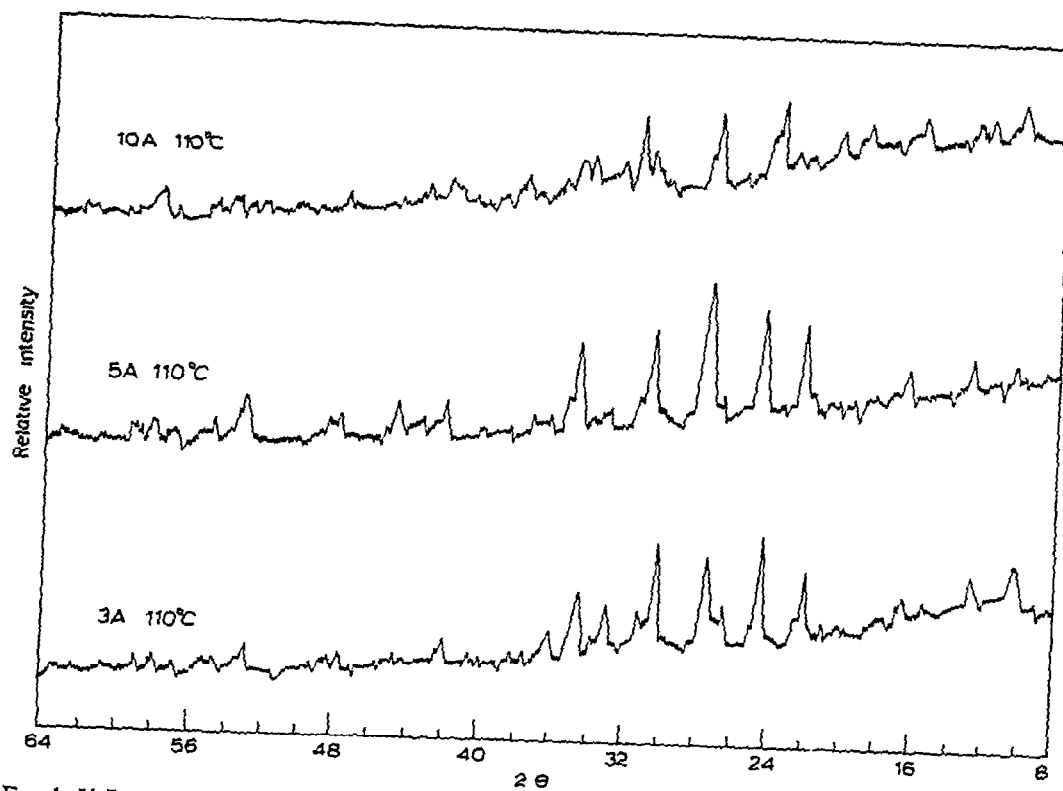


Fig 1 X-Ray diffraction patterns for 3, 5 and 10A zeolites thermally treated at 110°C

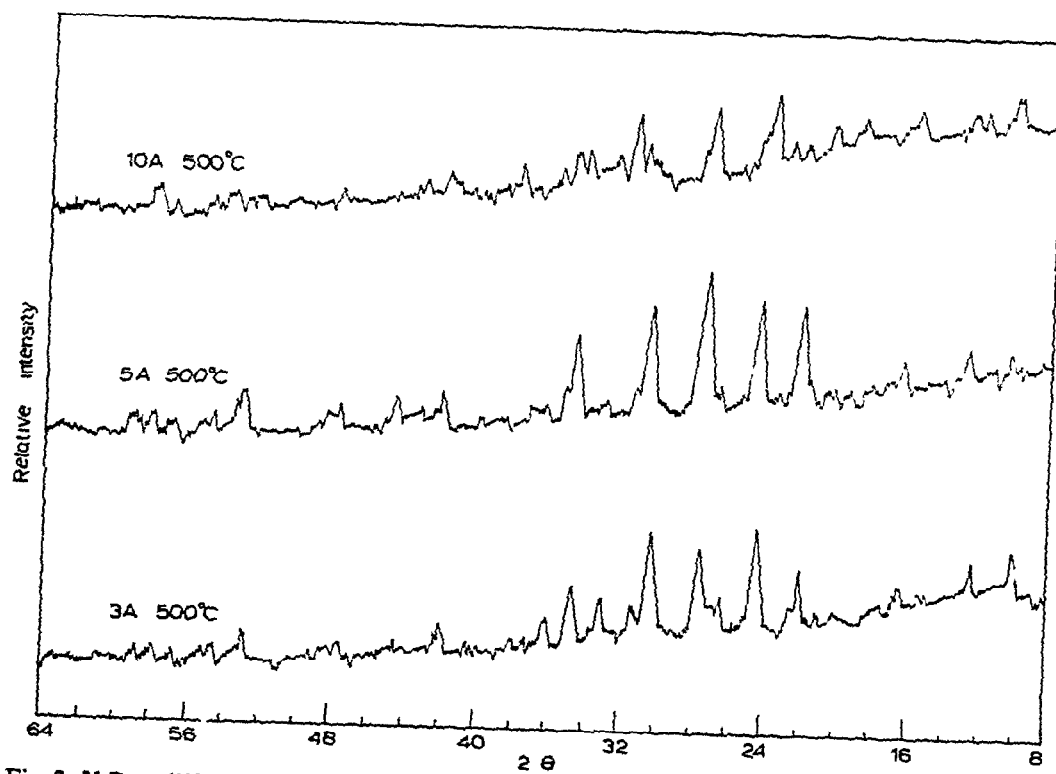


Fig. 2. X-Ray diffraction patterns for 3, 5 and 10A zeolites thermally treated at 500°C.

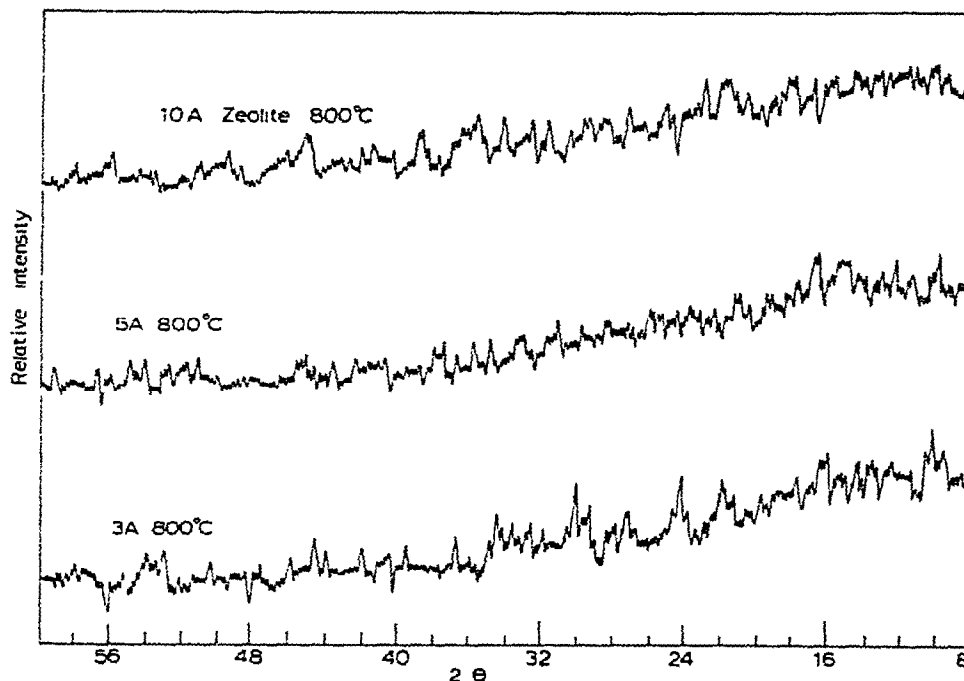


Fig 3 X-Ray diffraction patterns for 3, 5 and 10A zeolites thermally treated at 800°C

the main d values of 3.00, 4.18 and 3.27 Å at relative intensities of 100, 70 and 70, respectively. The diffraction patterns of the zeolites are maintained at 500°C and start to disappear upon heating at 800°C as shown in Fig. 3, thus indicating the occurrence of destruction of the zeolite lattice giving a matrix of different sintered oxides.

The DTA curves (Fig. 4) invariably exhibit one endothermic effect centered at 225, 250 and 225°C for 3, 5 and 10A zeolites, respectively, which may be correlated with the dehydration of loosely bound zeolitic water, and two successive exothermic effects, the former obtained at 855, 875 and 805°C and the latter centered at 920, 960 and 925°C for 3, 5 and 10A zeolites, respectively. The two exothermic effects may be correlated with the destruction of the zeolitic lattice which may occur in two steps; the first involving the removal of structural water, and the second involving breakdown of the lattice. Such thermal effects are demonstrated by the disappearance of the diffraction patterns of the zeolites upon heating at 800°C as shown in Fig. 3.

Thermogravimetric analysis was carried out in air and in vacuum for the three zeolite samples. The results obtained are graphically represented in Fig. 5a,b, where the % weight loss is plotted as a function of the increasing temperature in air and vacuum, respectively. Figure 6 represents differential thermogravimetric analysis (DTG) for 3, 5 and 10A zeolites in air in which $\Delta W/\Delta T$ is plotted as a function of increasing temperature. From TG and DTG analysis the following results can be summarized.

(a) For all samples effective dehydration appears to start at about 100°C for 3 and 5A zeolites and at $\sim 150^\circ\text{C}$ for 10A zeolite, and proceeds rapidly with the

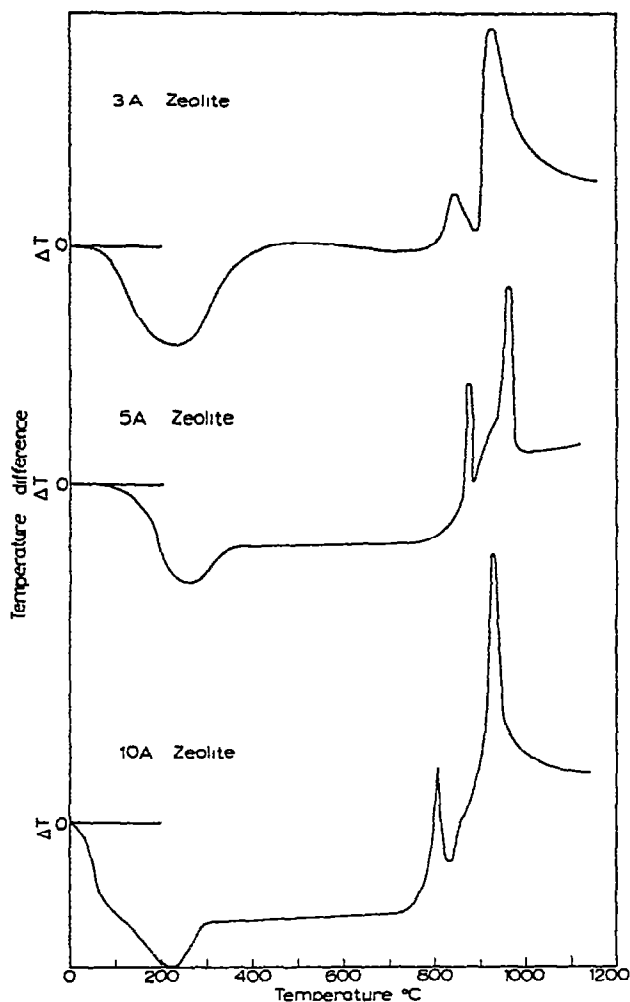


Fig 4 Differential thermal analysis curves for 3, 5 and 10A zeolites

regular increase in temperature up to about 300°C. Dehydration proceeds thereafter at a markedly slower rate and the tested samples attain a constant weight at about 350°C, whereby dehydration is effectively completed.

(b) Thermogravimetric analysis in air (Fig. 5a) indicates that the tested 3, 5 and 10A zeolite samples lost their zeolite water at % losses of 16.27, 12.17 and 6.48%, respectively, upon heating at about 360°C.

(c) DTG curves (Fig. 6) display a sharp peak centered at about 175, 175 and 225°C for 3, 5 and 10A zeolite, respectively. These values are correlated with the dehydration of zeolitic water.

(d) The observed water loss in air exceeds that in vacuum, an effect which may be attributed to contraction of pores that precedes the partial collapse of the zeolitic structure at elevated temperatures due to high vacuum procedure (cf. Fig. 5a,b).

Nitrogen adsorption-desorption isotherms obtained at -195°C on 3, 5 and 10A zeolites and their thermal products obtained at 100–1000°C are graphically illustrated in Figs. 7–9. Isotherms of the parent zeolites are of type I of the BDDT

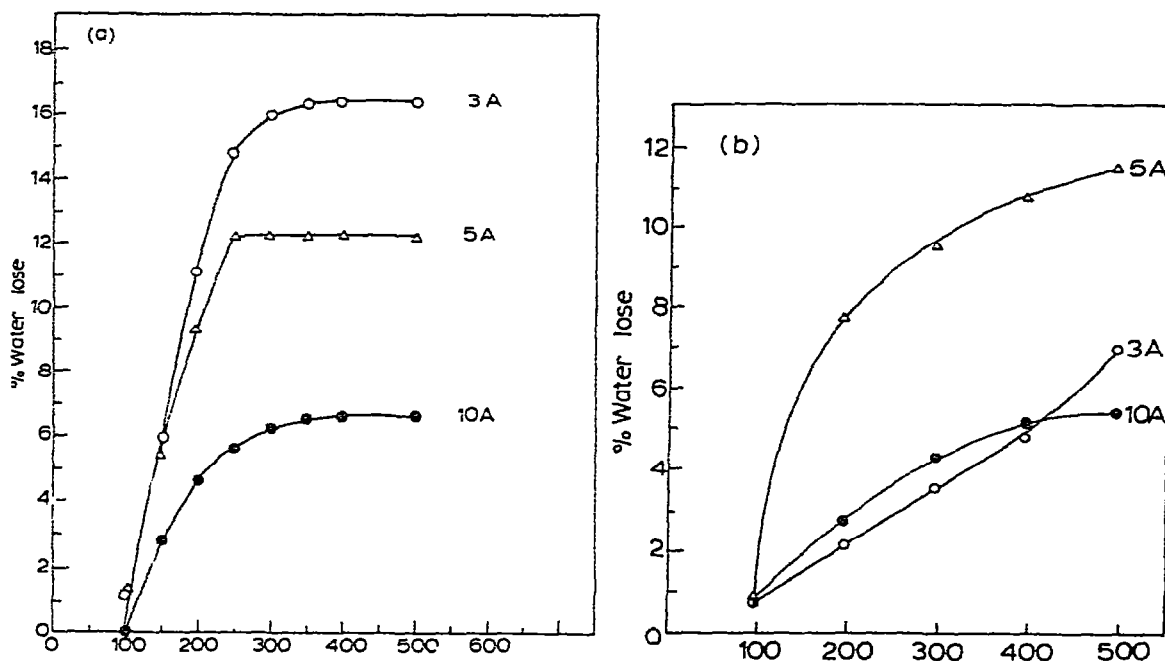


Fig 5 (a) Water loss ($\text{g } 100 \text{ g}^{-1}$) in air at various temperatures for parent 3, 5 and 10A zeolite samples (based on dry weight) (b) Water loss in vacuum as a function of temperature

classification [10], whereas those of samples thermally treated at $200\text{--}800^\circ\text{C}$ change to type II, and in the case of samples thermally treated at the highest temperature, viz. 1000°C , the isotherms change to type III.

Analysis of the nitrogen isotherms by the BET method [11], the monolayer capacity V_m , C-BET constant and specific surface area $S_{\text{BET}}^{\text{N}_2}$ were calculated by adopting 16.2 \AA^2 [12] as the cross-sectional area for the nitrogen molecule. The Dubinin Radushkevich method [13–15] was applied to various tested samples to

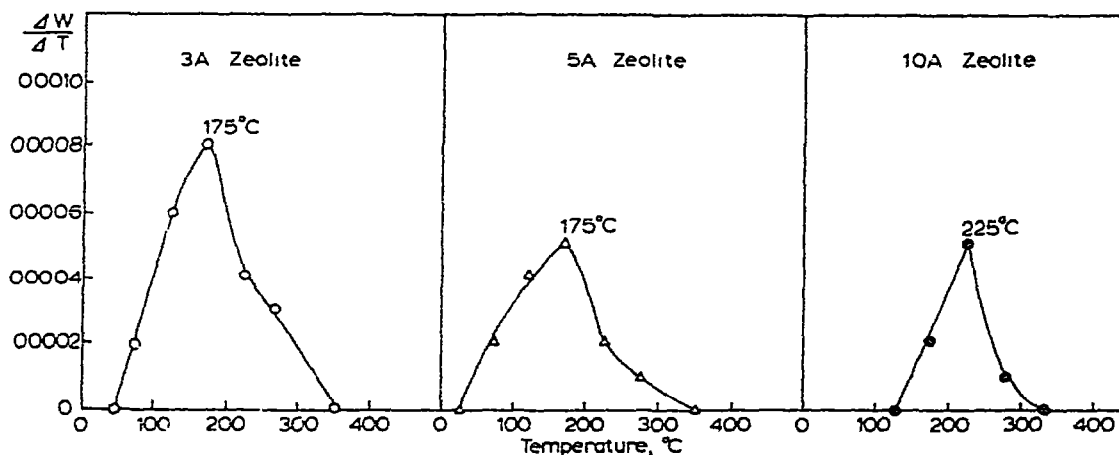


Fig 6 Differential thermogravimetric analysis curves for 3, 5 and 10A zeolites

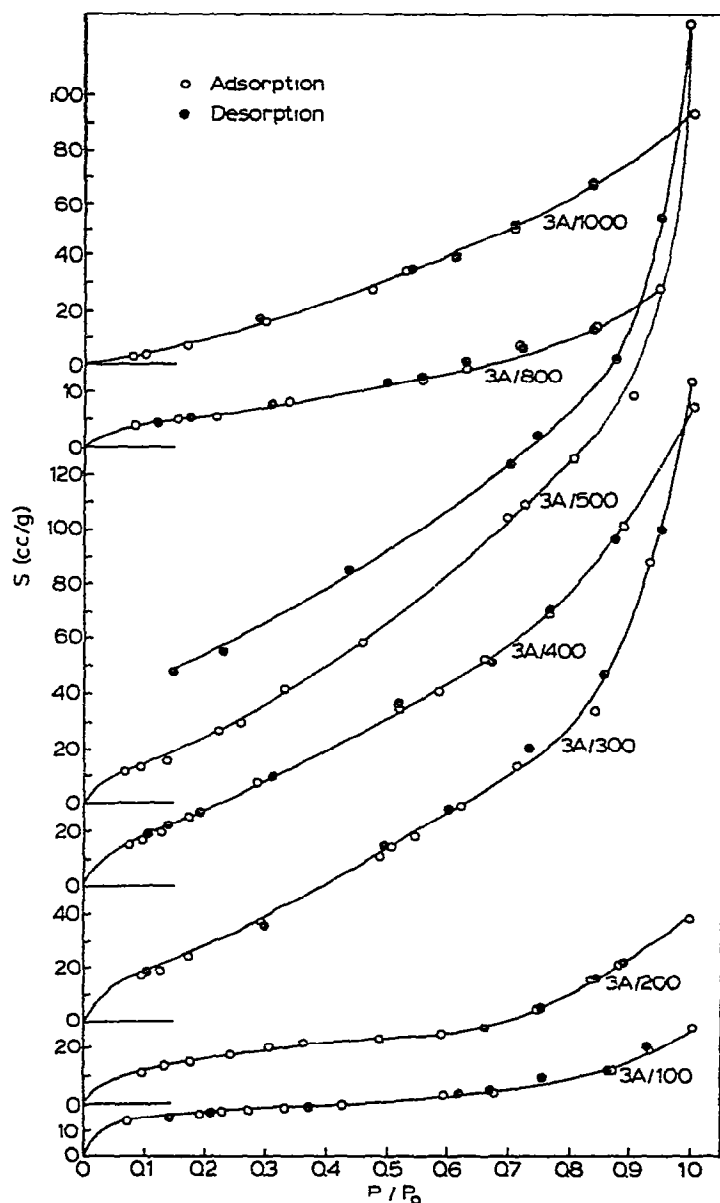


Fig 7 Adsorption-desorption isotherms of nitrogen on 3A zeolite thermally treated between 100 and 1000°C.

obtain the monolayer equivalent V_0^{DR} as shown in Figs. 10-12. The various surface parameters are summarized in Tables 1-3.

From the surface parameters obtained it can be seen that the monolayer equivalent, V_0^{DR} , calculated from the Dubinin Radushkevich equation is higher than the V_m values obtained from the BET method. This may be correlated with the influence of micropore filling in the low relative pressure region, leading to distortion in the shape of the isotherms in the early pressure region. Hence, evaluation of V_m from the

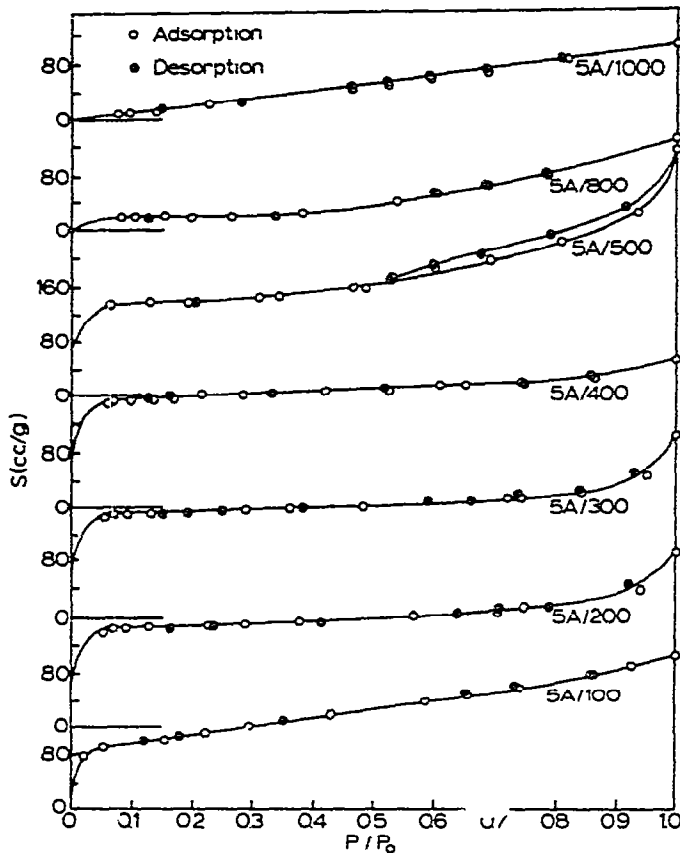


Fig 8 Adsorption-desorption isotherms of nitrogen on 5A zeolite thermally treated between 100 and 1000°C

BET equation is considered unreliable, particularly with the more microporous samples.

In general, the monolayer equivalent exhibits a distinct increase with increase in the pretreatment temperature up to 400°C, followed by a gradual decrease as the

TABLE I

Some surface characteristics from nitrogen adsorption data on 3A zeolite and its thermal dehydration products

Temp (°C)	Loss (%)	C-BET constant	V_m^{BET} ($\text{cm}^3 \text{g}^{-1}$)	S_{BET}^N ($\text{m}^2 \text{g}^{-1}$)	V_0^{DR} ($\text{cm}^3 \text{g}^{-1}$)	V_p (ml g^{-1})
100	0.85	101	13.2	58	19.2	0.0750
200	2.25	13	15.4	67	22.9	0.1070
300	3.65	11	28.3	124	41.7	0.3780
400	4.92	10	30.1	131	40.7	0.2720
500	7.16	11	26.7	117	22.9	0.4460
800	10.52	13	6.2	27		0.0460
1000				Type III		0.1460

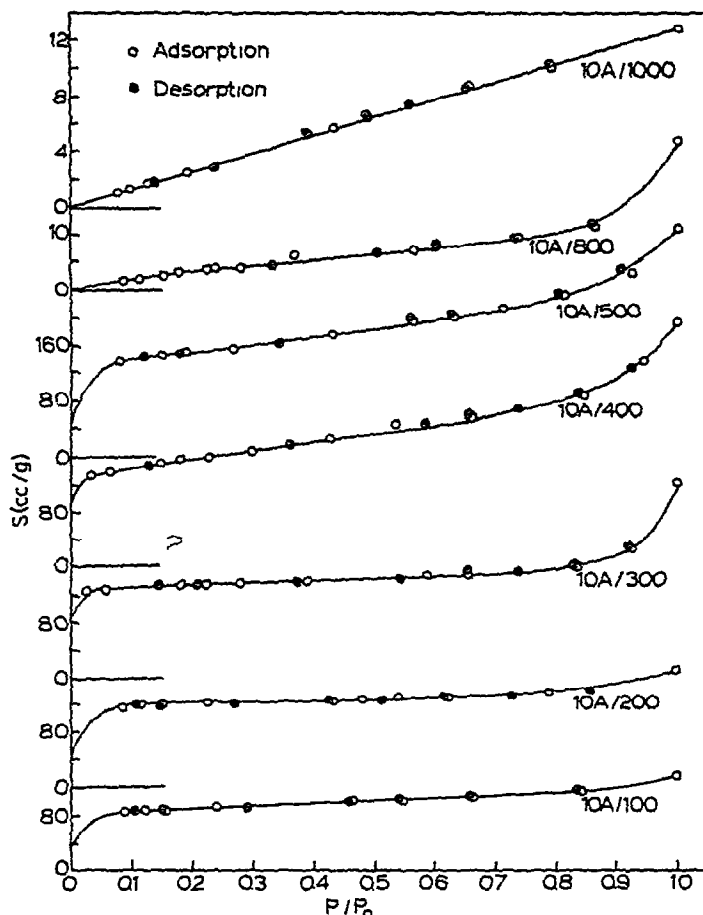


Fig 9. Adsorption-desorption isotherms of nitrogen on 10A zeolite thermally treated between 100 and 1000°C.

pretreatment temperature further increases. The first increase in the monolayer equivalent may be correlated with the removal of loosely bound water molecules held in the intracrystalline pores of the zeolite samples, an effect which leads to an increase in the accessibility of the nitrogen molecule in such pores. The optimum

TABLE 2

Some surface characteristics from nitrogen adsorption data on 5A zeolite and its thermal dehydration products

Temp (°C)	Loss (%)	C-BET constant	V_m^{BET} ($\text{cm}^3 \text{g}^{-1}$)	S_{BET}^N ($\text{m}^2 \text{g}^{-1}$)	V_0^{DR} ($\text{cm}^3 \text{g}^{-1}$)	t_p (ml g^{-1})
100	0.88	53	93.5	407	120	0.332
200	7.90	76	131.6	574	151	0.390
300	9.58	101	132.0	575	160	0.410
400	10.83	141	141.8	618	168	0.326
500	11.49	81	123.5	538	148	0.539
800	12.12	3	24.4	106		0.202
1000				Type III		0.168

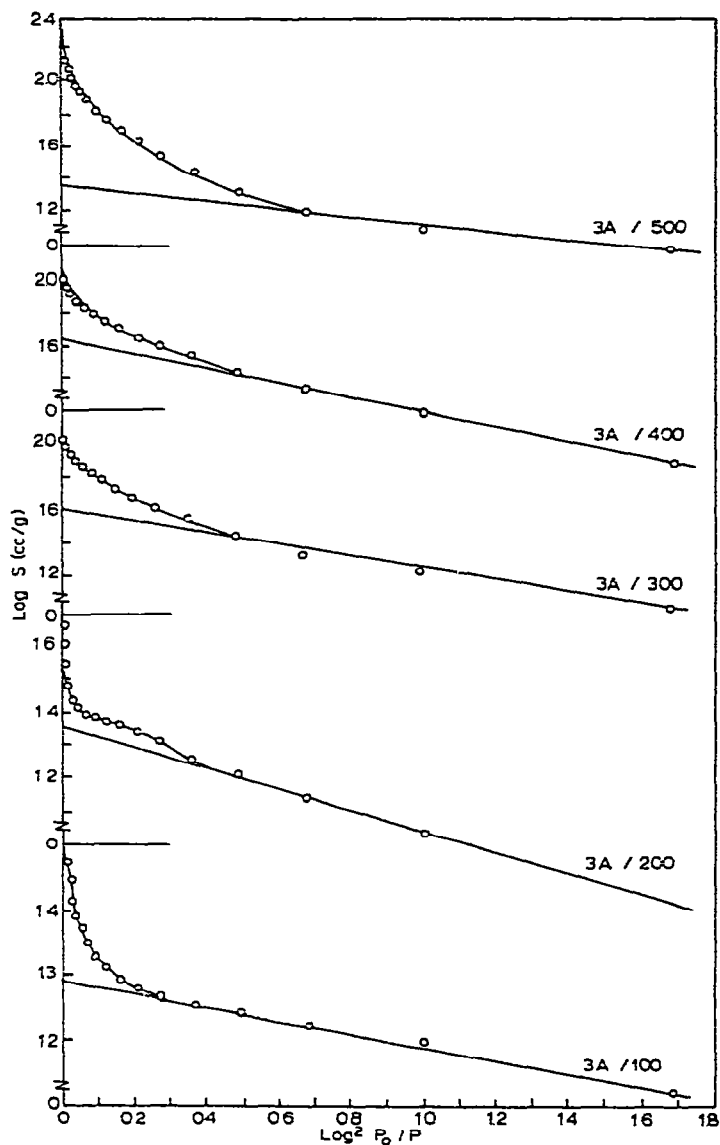


Fig 10 DR plots of nitrogen adsorption on 3A zeolite thermally treated between 100 and 500°C

TABLE 3

Some surface characteristics from nitrogen adsorption data on 10A zeolite and its thermal dehydration products

Temp (°C)	Loss (%)	C-BET constant	V_m^{BET} ($\text{cm}^3 \text{g}^{-1}$)	$S_{\text{BET}}^{\text{DR}}$ ($\text{m}^2 \text{g}^{-1}$)	V_0^{DR} ($\text{cm}^3 \text{g}^{-1}$)	V_p (ml g^{-1})
100	0.92	66	76	330	96	0.205
200	2.81	96	104	454	127	0.267
300	4.32	91	110	479	139	0.440
400	4.95	48	140	610	170	0.550
500	5.48	81	124	538	153	0.509
800	6.94	4	5.0	23		0.042
1000		4	4.0	19		0.020

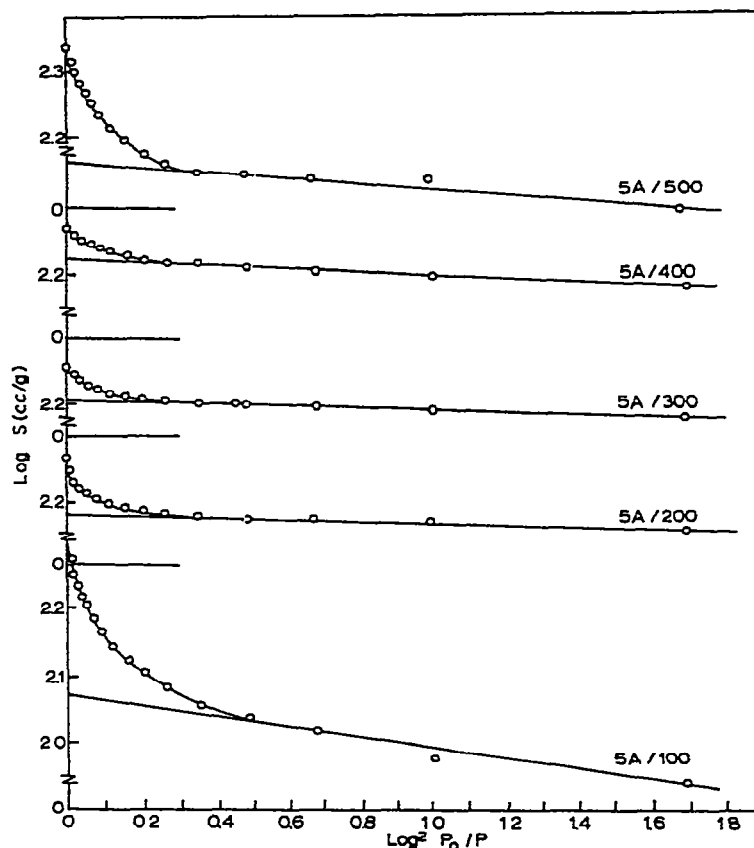


Fig 11 DR plots of nitrogen adsorption on 5A zeolite thermally treated between 100 and 500°C

temperature, at which maximum activation is attained, is 400°C. Further increasing the temperature leads to contraction of the pores, an effect which is accompanied by a decrease in the monolayer equivalent. Thermal treatment at 800–1000°C produced a marked diminution in the monolayer equivalent due to destruction of the zeolite lattice as shown by X-ray analysis (Fig. 3) at these elevated temperatures, producing a matrix of highly sintered oxides which differ in chemical nature and location from zeolites. This is also manifested in the change of type III nitrogen isotherms. The highest monolayer equivalents were obtained for 5A zeolite followed by 10A zeolite, then 3A zeolite. The lowest monolayer equivalents for 3A zeolites may be correlated with the inaccessibility of the nitrogen molecule (cross-sectional area 3.6 \AA^2) to 3A zeolite. On the other hand, 5 and 10A zeolites are accessible but the highest uptake of nitrogen was observed in the case of 5A zeolite due to the higher population of micropores in the case of 5A than in 10A zeolite. In conclusion, nitrogen adsorption isotherms can be used as a probe to follow the textural and structural changes in the tested zeolite samples which accompany thermal treatment.

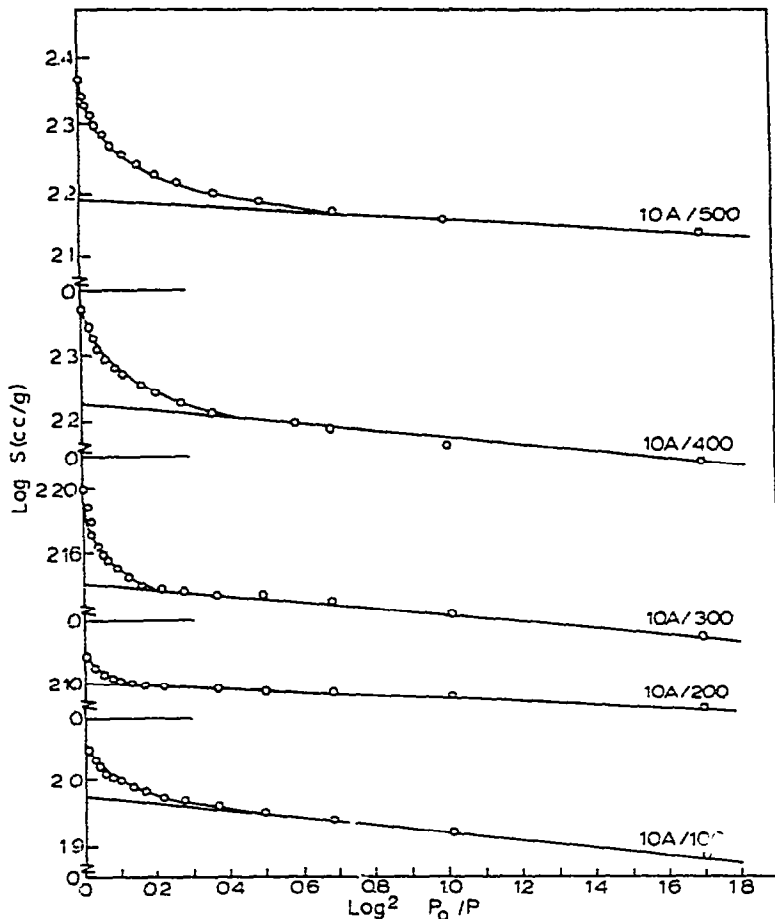


Fig 12 DR plots of nitrogen adsorption on 10A zeolite thermally treated between 100 and 500°C

REFERENCES

- 1 H W Habgood, Can J Chem, 36 (1958) 1384
- 2 V J Trilette, P B Weisz and A L Golden, J Catal, 1 (1962) 301
- 3 P B Weisz, V J Trilette, R W Matman and G B Mouser, J Catal, 1 (1962) 307
- 4 R M Milton, U.S. Patent 2, 882, 243-244, April 14 (1959)
- 5 D W Breck, W G Eversole and R M Milton, J Am Chem Soc, 78 (1956) 233
- 6 J V Smith (Ed), X-Ray Powder Data File and Index to the X-ray Powder Data File, 1961, ASTM, Philadelphia
- 7 R C MacKenzie, Differential Thermal Investigation of Clays, Mineralogical Society, London, 1957
- 8 H G McAdie, Anal Chem, 39 (4) (1967) 543
- 9 R I Razouk and A S Salem, J. Phys. Chem., 52 (1948) 1205
- 10 S Brunauer, L S Deming, W.E. Deming and E Teller, J Am Chem Soc, 62 (1940) 1723
- 11 S Brunauer, P.H Emmett and E. Teller, J. Am Chem Soc, 60 (1938) 309
- 12 D M Young and A D Crowell, Physical Adsorption of Gases, Butterworths, London, 1926, p 108
- 13 M M Dubinin and E.D Zaverian, Zh Fiz Khim, 23 (1949) 1129
- 14 L V Radushkevich, Zh Fiz Khim, 23 (1949) 1410
- 15 M M Dubinin, Chem Rev, 60 (1960) 235